Physica C 153–155 (1988) 590–593
North-Holland, Amsterdam

STUDIES OF SUPERCONDUCTING OXIDES WITH A SOLID-STATE IONIC TECHNIQUE

B.T. Ahn, T.M. Gür, and R.A. Huggins

Department of Materials Science and Engineering, Stanford University, Stanford, CA 94305.

R. Beyers, E.M. Engler, P.M. Grant, S.S.P. Parkin, G. Lim, M.L. Ramirez, K.P. Roche, J.E. Vazquez, V.Y. Lee, and R.D. Jacowitz

IBM Almaden Research Center, 650 Harry Road, San Jose, CA 95120-6099

This paper describes the use of a solid-state ionic technique to prepare $Y_1Ba_2Cu_3O_x$ samples with precisely controlled oxygen contents and to determine the Y-Ba-Cu-O quaternary phase diagram in the vicinity of $Y_1Ba_2Cu_3O_x$.

1. INTRODUCTION

Solid-state electrolytes such as yttria-stabilized-zirconia provide unmatched precision in their ability to both control and monitor oxygen pressure. Moreover, they provide one of the fastest, most accurate methods to determine phase equilibria in multicomponent oxide systems (1). Herein, we describe the application of a solid-state ionic technique to two problems in superconducting oxides: the preparation of low-oxygen content $Y_1Ba_2Cu_3O_x$ samples with well-defined processing histories (2) and the determination of the Y-Ba-Cu-O quaternary phase diagram in the vicinity of $Y_1Ba_2Cu_3O_x$ (3). The first problem is of interest because of the conflicting reports which have appeared regarding the structure and properties of low-oxygen content $Y_1Ba_2Cu_3O_x$ samples. For example, Johnston *et al.* (4) found samples prepared by interdiffusing mixtures of $Y_1Ba_2Cu_3O_6$ and $Y_1Ba_2Cu_3O_7$ in sealed silica tubes to be tetragonal and not superconducting below $Y_1Ba_2Cu_3O_{6.5}$, whereas Cava *et al.* (5) found samples prepared by a zirconium gettering technique to be orthorhombic with a large superconducting volume fraction at $Y_1Ba_2Cu_3O_{6.30}$. The second problem is of interest because the technological usefulness of $Y_1Ba_2Cu_3O_x$ will depend in part on its thermodynamic stability over the range of temperatures and oxygen pressures to which it is exposed during its fabrication and use.

2. EXPERIMENT

The solid-state ionic cell used consisted of a closed quartz chamber with two interconnected compartments, as shown schematically in Fig. 1. Each compartment had its own furnace for independent temperature control. One compartment contained the Y-Ba-Cu-O sample. A nearby thermocouple monitored the thermal history of the sample, including the quenching process. The other compartment housed a yttria-stabilized-zirconia (YSZ) solid electrolyte tube, closed at one end, with porous platinum electrodes deposited on the inner and outer walls at the closed end. The interior of the YSZ tube was exposed to ambient air, to act as an oxygen reference electrode.

The YSZ tube served two purposes. Under open circuit conditions, it acted as an oxygen sensor to monitor the oxygen pressure inside the sealed chamber. Under DC-biased conditions, it served as an oxygen "pump" to quantitatively titrate oxygen into or out of the chamber and to maintain a desired level of oxygen pressure within the chamber. The YSZ compartment was operated at a fixed temperature of 850 °C to obtain high ionic conductivity and thus rapid oxygen transport.

The samples with reduced oxygen content were prepared in the following manner. $Y_1Ba_2Cu_3O_{7.00}$ starting material [oxygen content derived from iodometric titration (6)] was placed in an alumina boat in the chamber and heated to 500 °C. During the temperature ramp up, enough oxygen was pumped out of the chamber to ensure that the total pressure remained below 1 atm. At 500 °C, oxygen was titrated out of the chamber for 2 - 3 days. The sample remained at 500 °C for an additional day after the desired oxygen content was attained. The sample was then either air quenched to 25 °C by removing the furnace around the sample compartment or slowly cooled by stepping down the sample furnace temperature to 25 °C over a 28 hour period.

The oxygen content in the reduced samples was derived from the known starting composition and the measured weight change in the sample (total sample weight ~10 grams). This value was checked by performing iodometric titration on small portions of each sample. Based on the results of these two methods, we estimate that the quoted oxygen contents are accurate to within ±0.02 oxygens per formula unit.

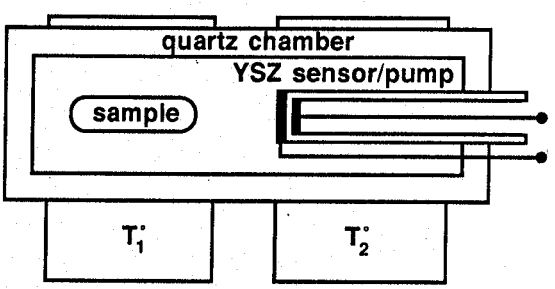

Figure 1. Schematic of the apparatus.

0921–4534/88/$03.50

For the phase equilibria studies, two compositions with different cation ratios were studied. Sample 1 was single-phase $Y_1Ba_2Cu_3O_x$. Sample 2 had the nominal composition $Y_2Ba_{2.5}Cu_{5.5}O_x$ and was a mixture of the $Y_1Ba_2Cu_3O_x$, Y_2BaCuO_5, and CuO phases.

Oxygen coulometric titration experiments were carried out to obtain phase equilibria data (7). This involved titration of known small amounts of oxygen out of the sealed chamber by passage of current under potentiostatic conditions at about 1 volt. The current was subsequently interrupted and the system was allowed to equilibrate. The equilibration process was continuously monitored by observing the open circuit potential of the oxygen sensor on a strip chart recorder until a constant value was reached. This procedure was repeated to establish the coulometric titration curve for the oxygen composition-oxygen pressure relationship.

X-ray diffraction and transmission electron microscopy (TEM) were used for structural characterization of all of the samples. Resistivity, thermopower, and susceptibility measurements were used to determine the superconducting properties of the low-oxygen content samples.

3. RESULTS

3.1. Structure and properties of low-oxygen content $Y_1Ba_2Cu_3O_x$ samples

Samples with oxygen contents of 6.14, 6.30, 6.41, 6.50, and 6.61 were prepared and examined.

X-ray diffraction indicated that the slowly cooled $Y_1Ba_2Cu_3O_{6.14}$ and $Y_1Ba_2Cu_3O_{6.30}$ samples were tetragonal. Resistively, both sample were insulators. Because the results on the $Y_1Ba_2Cu_3O_{6.30}$ sample appear to contradict those of Cava *et al.*(5), we prepared an air quenched $Y_1Ba_2Cu_3O_{6.30}$ sample to see if a variation in the quench rate could explain the difference. The air quenched sample also was tetragonal and an insulator, although magnetometry data indicated approximately 0.2% of this sample was superconducting below ~30 K. Electron diffraction studies of individual crystals found the air quenched sample to be tetragonal, with no twins present in the microstructure. A few crystals, however, did exhibit a feint, tweed-like microstructure, as if on the verge of transforming to the orthorhombic structure.

The quench rate did affect the structure and properties of the $Y_1Ba_2Cu_3O_{6.41}$ samples. Both the slowly cooled and air quenched samples were orthorhombic (Fig 2). However, the (200) and (020) x-ray diffraction peaks in the slowly cooled sample were sharper and more clearly separated than those in the air quenched sample, indicating greater oxygen ordering in the slowly cooled sample. Greater oxygen ordering in the slowly cooled samples was also evident in the electron diffraction patterns: weak superlattice spots halfway between reflections along the a* axis, corresponding to a doubling of the a axis in the unit cell, were much sharper in the slowly cooled sample. (These spots probably arise from the ordered removal of oxygen from every other CuO "linear chain" in samples with oxygen contents near 6.5.) Despite its greater oxygen order, the slowly cooled material had a lower transition temperature than the air quenched material. The slowly cooled sample had a higher resistivity over the entire temperature range studied and it did not reach zero

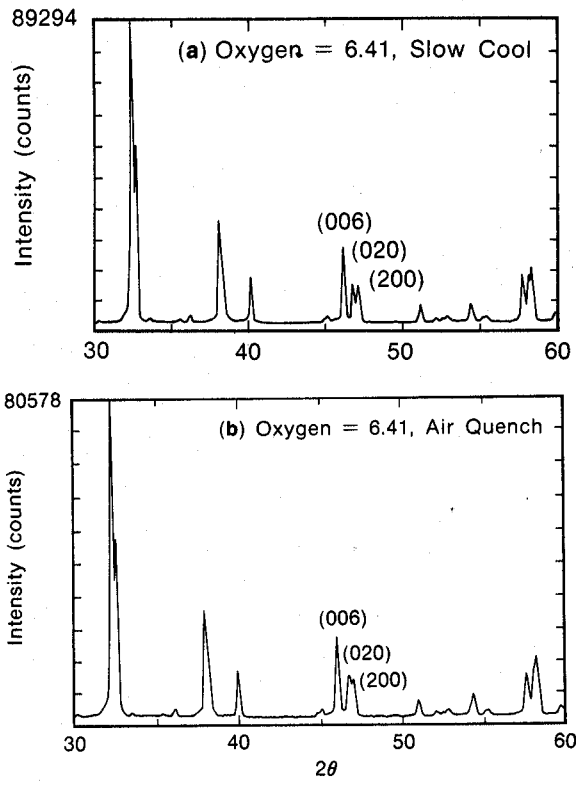

Figure 2. X-ray diffraction patterns for oxygen 6.41 samples (a) slow cooled and (b) air quenched from 500 °C.

resistance down to 4 K (Fig. 3). Figure 4 compares the shielding data in the two samples. Diamagnetic shielding was only 0.2% and 2% of that expected for a perfect diamagnet in the slowly cooled and air quenched samples, respectively, indicating that neither of these samples was a bulk superconductor. We interpret the slope changes in both the shielding and resistivity data of the air quenched sample as evidence for local regions in the material with critical temperatures of 30, 50, and 80 K. It is reasonable to suggest that local inhomogeneities in the oxygen content of this sample gave rise to these superconducting regions. We currently believe these inhomogeneities were caused by stress induced diffusion during the quench, with the stresses arising from the thermal expansion anisotropy in $Y_1Ba_2Cu_3O_x$. By comparison, the shielding data for the slowly cooled sample indicated only trace amounts of material with a critical temperature of 50 K (not observable in Fig. 4) and somewhat larger regions with a critical temperature of 10 K (arrowed in Fig. 4).

The orthorhombic distortion and the superconducting transition temperature increased in samples with even greater oxygen content, as expected. The superlattice spots in electron diffraction patterns of the $Y_1Ba_2Cu_3O_{6.50}$ sample were much sharper and stronger than those in the $Y_1Ba_2Cu_3O_{6.41}$ sample. The zero resistance temperatures for slowly cooled $Y_1Ba_2Cu_3O_{6.50}$ and $Y_1Ba_2Cu_3O_{6.61}$ samples were 37 and 56 K, respectively.

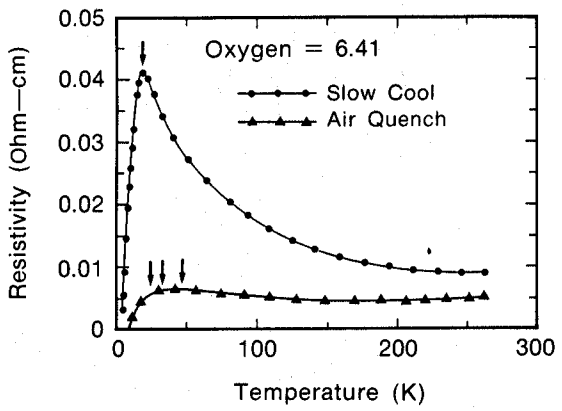

Figure 3. Resistivity versus temperature plots for oxygen 6.41 samples slow cooled (circles) and air quenched (triangles) from 500 °C.

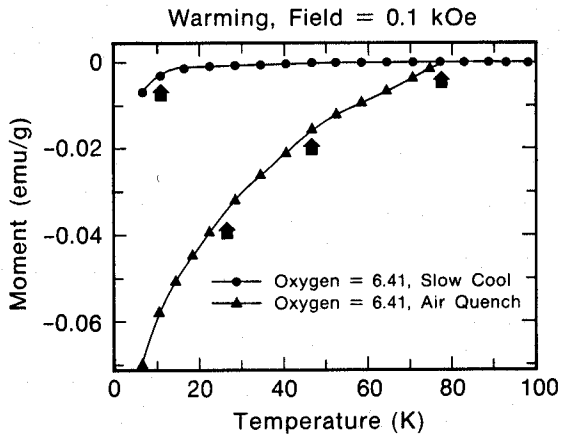

Figure 4. Enlarged plot of shielding data for slow cooled $Y_1Ba_2Cu_3O_{6.41}$ and air quenched $Y_1Ba_2Cu_3O_{6.41}$ samples. The arrows point out slope changes. Corresponding changes are marked in Figure 3.

3.2. Phase equilibria in the vicinity of $Y_1Ba_2Cu_3O_x$

Figure 5 shows the oxygen coulometric titration curves at 850 °C for Samples 1 and 2.

For Sample 1, the equilibrium oxygen pressure monotonically decreased in the single phase region from 0.21 atm to 1 x 10^{-3} atm of oxygen pressure with increasing reduction in the oxygen content. In this region the presence of two slight kinks was observed. However, the cause and the nature of these kinks have not yet been resolved. The equilibrium oxygen pressure reached a plateau value at 1 x 10^{-3} atm, indicating the presence of an invariant polyphase reaction in accordance with the Gibbs phase rule. This finding has important implications for the thermodynamic stability of $Y_1Ba_2Cu_3O_x$. It indicates that $Y_1Ba_2Cu_3O_x$ undergoes a decomposition reaction and is thermodynamically unstable below 1 x 10^{-3} atm of oxygen pressure at this temperature.

One batch of Sample 1 was equilibrated just above plateau I at 3.7 x 10^{-2} atm of oxygen pressure, while another batch of Sample 1 was equilibrated just below the plateau at 5.2 x 10^{-4} atm. X-ray diffraction indicated the sample equilibrated above plateau I contained only the tetragonal phase $Y_1Ba_2Cu_3O_x$, whereas the sample equilibrated below plateau I contained Y_2BaCuO_5, $BaCuO_2$ and Cu_2O, but not $Y_1Ba_2Cu_3O_x$. Hence plateau I represents the co-existence of $Y_1Ba_2Cu_3O_x$, Y_2BaCuO_5, $BaCuO_2$ and Cu_2O at 1 x 10^{-3} atm of oxygen pressure at 850 °C.

For Sample 2, the oxygen pressure decreased monotonically until a plateau at 4.1 x 10^{-3} atm was reached. At this plateau, labelled II in Figure 5, CuO decomposes into Cu_2O. The oxygen pressure for the CuO/Cu_2O equilibrium measured here is in excellent agreement with established thermochemical data (8). Decreasing the oxygen pressure below this plateau leads again to plateau I at 1 x 10^{-3} atm of oxygen pressure, in agreement with the results from Sample 1. Again, the presence of this plateau indicates an invariant point where the four phases $Y_1Ba_2Cu_3O_x$, Y_2BaCuO_5, $BaCuO_2$ and Cu_2O coexist. With further reduction, plateau III is reached at 1.9 x 10^{-5} atm of oxygen pressure. X-ray diffraction analysis of a batch of Sample 2 equilibrated at 5.4 x 10^{-5} atm of oxygen pressure, just above plateau III, indicated the presence of three phases, Y_2BaCuO_5, $BaCuO_2$ and Cu_2O. This evidence independently confirmed that the tetragonal $Y_1Ba_2Cu_3O_x$ phase is thermodynamically stable down to 1 x 10^{-3} atm of oxygen pressure at 850 °C.

Based on the titration and x-ray diffraction data, a portion of the Y-Ba-Cu-O quaternary phase diagram near the $Y_1Ba_2Cu_3O_x$ composition was constructed (Fig. 6). For simplicity, each phase is treated as a point compound in the diagram and solid lines represent two-phase tie-lines. Within each sub-tetrahedron, the four phases represented by the corner compositions are in equilibrium with each other. At constant temperature and total pressure, the Gibbs phase rule can be expressed as F = C - P where F, C, and P represent the degrees of freedom, number of components, and number of phases, respectively. For each subtetrahedron, P = C = 4 and hence F = 0. Under these circumstances, the compositions of phases are fixed and

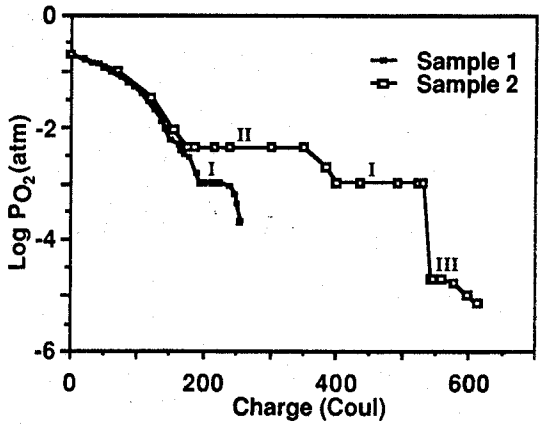

Figure 5. Oxygen coulometric titration curves for Samples 1 and 2 at 850 °C.

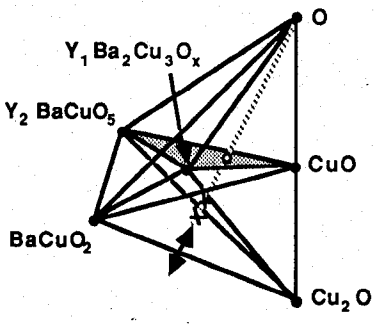

Figure 6. Three-dimensional quaternary phase diagram at 850 °C around $Y_1Ba_2Cu_3O_x$. Solid lines indicate the tie-lines and the hatched area indicates the triangle in which the starting composition for Sample 2 resides.

cannot be varied at will. Consequently, the equilibrium oxygen pressure within each subtetrahedron is fixed at a constant value: the oxygen pressure in the $Y_1Ba_2Cu_3O_x$-Y_2BaCuO_5-$BaCuO_2$-Cu_2O subtetrahedron is just the plateau I pressure, whereas the equilibrium pressures in the $Y_1Ba_2Cu_3O_x$-Y_2BaCuO_5-CuO-Cu_2O and $Y_1Ba_2Cu_3O_x$-$BaCuO_2$-CuO-Cu_2O subtetrahedra are governed by the CuO/Cu_2O equilibrium pressure (plateau II).

Figure 7 shows the variation of the $Y_1Ba_2Cu_3O_x$ decomposition pressure and CuO/Cu_2O equilibrium pressure with reciprocal temperature (9). $Y_1Ba_2Cu_3O_x$ is thermodynamically stable above the plateau I line, but it is unstable below this line. Extrapolation of the two lines to lower temperatures indicates that they may intersect. If this occurs, then $Y_1Ba_2Cu_3O_x$ would undergo a eutectoid decompostion reaction at the temperature at which the two lines meet. Moreover, $Y_1Ba_2Cu_3O_x$ would be thermodynamically unstable below this temperature. Sluggish kinetics, however, would probably prevent this invariant reaction from being observed in practice.

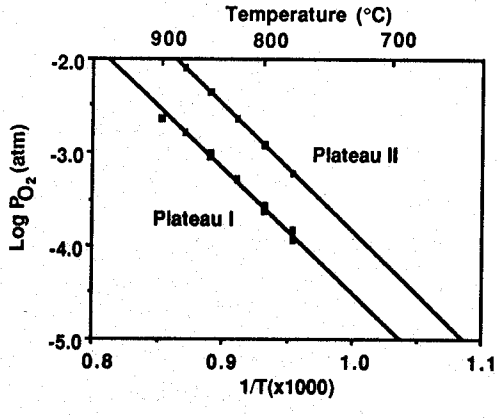

Figure 7. Oxygen pressures for $Y_1Ba_2Cu_3O_x$ decomposition and for CuO/Cu_2O equilibrium between 700 and 900 °C. Below ~ 700 °C, the data exhibit poor reproducibility due to sluggish kinetics.

4. CONCLUSIONS

In this work, like Cava *et al.* (5), we find that orthorhombic $Y_1Ba_2Cu_3O_{9-x}$ material with oxygen content below 6.5 can be prepared by low-temperature removal of oxygen from $Y_1Ba_2Cu_3O_{7.00}$. For oxygen removal at 500 °C, however, we find that the orthorhombic phase cannot be retained down to $Y_1Ba_2Cu_3O_{6.30}$. Lower titration temperatures may extend the oxygen stoichiometry range of the orthorhombic phase. Our results indicate that oxygen inhomogeneities are essential for observing small amounts of superconductivity in $Y_1Ba_2Cu_3O_{9-x}$ samples with oxygen contents below 6.5. This conclusion supports the view that a high oxidation state in the copper-oxygen network, whether on a local scale (inhomogeneities in $Y_1Ba_2Cu_3O_{<6.5}$ samples) or on a global scale ($Y_1Ba_2Cu_3O_{>6.5}$ samples), is essential for high-temperature superconductivity.

Oxygen coulometric titration has been used to determine the stability of $Y_1Ba_2Cu_3O_x$ for a wide range of oxygen pressures and temperatures and to construct a portion of the Y-Ba-Cu-O phase diagram.

The solid-state ionic method described here enables complete control of both the thermal history of the sample and its oxygen environment. It can be readily used for well-defined studies of other samples of interest, including $Y_1Ba_2Cu_3O_x$ single crystals and the plethora of oxide structures found to exhibit high-temperature superconductivity.

ACKNOWLEDGEMENTS

Financial support from the U.S. Department of Energy under subcontract LBL-4536310 is gratefully acknowledged.

REFERENCES

(1) W. Weppner, Chen Li-chuan, and W. Piekarczyk, Z. Naturforsch. **35a** (1980) 381.
(2) R. Beyers, E.M. Engler, P.M. Grant, S.S.P. Parkin, G. Lim, M.L. Ramirez, K.P. Roche, J.E. Vazquez, V.Y. Lee, R.D. Jacowitz, B.T. Ahn, T.M. Gür, and R.A. Huggins, Mater. Res. Soc. Symp. Proc. **99** (1988) in press.
(3) B.T. Ahn, T.M. Gür, R.A. Huggins, R. Beyers, and E.M. Engler, Mater. Res. Soc. Symp. Proc. **99** (1988) in press.
(4) D.C. Johnston, A.J. Jacobson, J.M. Newsam, J.T. Lewandowski, D.P. Goshorn, D. Xie, and W.B. Yelon, ACS Symposium Series **351**: Chemistry of High Temperature Superconductors, (1987) 136.
(5) R.J. Cava, B. Batlogg, C.H. Chen, E.A. Rietman, S.M. Zahurak, and D. Werder, Phys. Rev. B **36** (1987) 5719.
(6) A.I. Nazzal, V.Y. Lee, E.M. Engler, R.D. Jacowitz, Y. Tokura, and J.B. Torrance, this volume.
(7) W. Weppner and R.A. Huggins, J. Electrochem. Soc. **125** (1978) 7.
(8) I. Barin and O. Knacke, Thermochemical Properties of Inorganic Substances, (Springer-Verlag, 1973).
(9) This figure includes data obtained shortly after the Interlaken meeting. This new data indicates that the two lines intersect at a much lower temperature than reported at the conference, if at all.